The Islamic University of Gaza

Deanery of Higher Studies

Faculty of Science

Department of Physics

THEORY OF MAGNETOSTATIC SURFACE WAVES ON LEFT-HANDED MATERIALS (LHM)

Presented By

Shawqi A. Qader Moh'd Mansour

Supervised By

Prof. M. M. Shabat

Submitted in Partial Fulfillment of the Requirements for the Degree of Master of Science

Gaza Strip, Gaza

Palestine

2006

To

my parents for their kind help,

my wife,

Om-Hamza

and my sons,

Hamza, Moaz, Jafar, Ilaf, Arwa, Omar.

ACKNOWLEDGEMENTS

I wish to express my profound gratitude to my supervisor professor M. M. Shabat for his encouragement and guidance offered me throughout this thesis.

I express my deep gratitude to Dr. Majdi S. Hamada from department of physics at Al-Aqsa University for continuous helpful discussions and comments during this work.

Also, I sincerely thank all members of my family for their continuous support and encouragement.

Finally, sincere thanks are due to all of my colleges in the physics department at Islamic University of Gaza (IUG).

CONTENTS

CHAPTER (3)
Nonlinear magnetostatic surface waves in a LHM

CHAPTER (4)
Numerical Analysis

Abstract

During the last few years, several investigations and studies have been carried out on both nonlinear behavior of electromagnetic waves and nonlinear magnetostatic surface waves. Recently, new artificial left handed materials (LHMs) have been fabricated, where both permittivity and permeability are negative.

These materials (LHM's) have become important, because of its scattering to the electromagnetic radiation in a unique manner and some useful applications, for example, uses in the cellular communications industry, antennas, filtering, and other electromagnetic devices are of great importance.

In this dissertation we investigate the properties of the dispersion of nonlinear magnetostatic surface waves in LHM / ferrite structure. Maxwell's equations and the boundary conditions have been used to derive the dispersion relation.

Numerical and analytical approaches are implemented in order to find out the characteristics of the nonlinear magnetostatic surface waves. The guiding structure we considered consists of a linear gyromagnetic ferrite and left-handed material. Numerical results are also illustrated. Obtained results could be used in designing some future electromagnetic devices.

Introduction

Vector Veselago in his paper [1] published in 1968, postulated a material in which both permittivity and permeability had negative real values, and he showed theoretically that in such a medium, which he called “Left-Handed (LH)” medium, the wave vector is antiparallel to the usual right-handed cross product of the electric and magnetic fields, implying effectively negative refractive index for such a medium.

Smith and his colleagues [2] in recent years have constructed a composite medium with such features in the microwave regime, by arranging arrays of small metallic wires and split ring resonator and have shown the anomalous “negative” refraction predicted by Veselago.

Various features of this class of metamaterials, also known as “double negative (DNG)” media, and many ideas and suggestions for their potential applications are now being studied by many researchers [1-12].

In this thesis, the nonlinear magnetostatic surface waves propagating along two various media containing a linear ferrite substrate and a left-handed material cover have been studied. Maxwell’s equations and the boundary conditions have been used to derive the dispersion equation. The outline of this thesis is classified into four chapters.

Chapter 1 describes an introductory development of both the nonlinear magnetostatic surface waves propagation along layered structures, and the important properties and characteristics of LHM's.

Chapter 2 presents TE surface waves along a single interface of semi-infinite linear ferrite (ε_f = 1) and vacuum with ($\varepsilon_0 = \mu_0 = 1$). The dispersion relation has been solved to find out the nonreciprocal nature of the propagation.

Chapter 3 examines the behavior of nonlinear magnetostatic surface waves on two layers containing ferrite (YIG) and left-handed material.

Chapter 4 includes analytical and numerical solution of the dispersion relation which was derived in the previous chapter.

1.1 Historical development

Magnetostatic surface wave technology is widely used in practical sophisticated devices for direct signal processing, such as bandpass filters, resonators filters, oscillators, and circulators. Magnetostatic surface wave, whose wavenumber lies in the range between electromagnetic waves and exchange spin waves, was first considered theoretically (Damon and Esbach 1961) in a gyromagnetic ferrite slab [Yttrium Iron Garnet (YIG)] magnetized in the plane of its faces, propagating in a direction transverse to the applied static magnetic field [12].

Magnetostatic surface waves on different magnetic layered structures have been investigated in the voigt geometry by several researchers (Lax and Button 1962, Sodha and Srivastava 1981) [13].

Shabat [13] has computed the dispersion relation of strongly nonlinear magnetostatic surface waves in a grounded ferrite (YIG) film bounded by a nonlinear dielectric cover. It is found that the dispersion can be tuned and controlled by selecting the film thickness in both directions of propagation, where non-reciprocity is obtained. The effect of applied magnetization is also discussed.

The general dispersion relation for strongly nonlinear magnetostatic surface waves in a gyromagnetic (YIG) film is also analyzed theoretically by Shabat [14] and calculated for different values of the cover-film interface nonlinearity. The difference between the phase constants for forward and backward propagation direction against the film thickness has also been computed at different values of the signal operating frequency. It has been found that the differential phase constant or the non-reciprocity can be minimized for the smaller operating frequencies and relatively thick films.

1.2 Nonlinear electromagnetic waves

There is a considerable interest in the exact properties of strong electromagnetic waves propagating in layered structures in which one or more medium is nonlinear. Many weakly nonlinear guided wave optical devices have been proposed. This is based upon the concept that the intensity of the nonlinear guided or surface waves controls only the propagation wave index [15-17].

Bordman et al [18-19] have extended the study of the properties of strong nonlinear surface waves from infrared to down to microwave frequencies. They derived an exact theory of electromagnetic waves propagating along a single interface between a linear ferromagnetic substrate and a strongly nonlinear artificial paramagnetic cladding. The main conclusion is that both TE and TM waves can propagate even if such propagation is forbidden in the linear, low-power limit.

At the present time, little seems to be known about solutions of Maxwell's equations that describe the propagation of surface or guided waves in nonlinear structures that involve linear gyromagnetic media. In addition, almost all of the exact studies of TE and TM nonlinear surface waves or polaritons have been based on frequency-independent dielectric constants and attention has focused upon the infrared region of the spectrum [19, 22].

As a background in this chapter, we are going to review few important works which concerns with magnetostatic surface waves, LHM and a ferrite (YIG).

1.3 Strongly nonlinear magnetostatic surface waves in a grounded ferrite film

Shabat [14] has investigated theoretically the new strongly nonlinear magnetostatic surface waves in the Voigt configuration for a YIG substrate and nonlinear dielectric cover. The nonlinearity of the dielectric cover is much stronger than the weak nonlinearity of the YIG substrate, so that the weak nonlinearity of YIG can simply be neglected and the magnetostatic approximation will also be used. Waves will be in a direction transverse to the applied magnetic field. The properties of the dispersion of nonlinear magnetostatic surface waves in a grounded ferrite film were investigated. The new approach might be integrated and extended to study the amplification of nonlinear magnetostatic surface waves though their interaction with drifting carriers of the semiconductor.

The ferrite occupies the region $0 \le z \le d$ which is grounded at z = 0, bounded by the nonlinear cover of the space $z \ge d$. We present the dispersion equation for stationary TE waves propagating in the x-direction with propagation wave in the form exp [i(kx–2πft)]. The magnetic permeability tensor of the gyromagnetic ferrite (YIG) substrate is described as:

$$m(w) = \begin{pmatrix} m_{xx} & 0 & m_{xz} \\ 0 & m_B & 0 \\ -m_{xz} & 0 & m_{xx} \end{pmatrix} \tag{1.1a}$$

Where:

$$m_{xx} = m_B \left(\frac{w_0 (w_0 + w_m) - w^2}{w_0^2 - w^2} \right), \quad m_{xz} = i m_B \frac{w w_m}{w_0^2 - w^2} \tag{1.1b}$$

and μ_B is the usual Polder tensor elements,

ω is the angular frequency of the supported wave,

$\omega_0 = \gamma\mu_0 H_0$, $\omega_m = \gamma\mu_0 M_0$, H_0 is the applied magnetic field,

$\gamma = 1.76\times10^{11}$ $S^{-1}T^{-1}$ is the gyromagnetic ratio,

M_0 is the dc saturation magnetization of the magnetic insulator and μ_B has been introduced as the background, optical magnon permeability.

The ferrite has also a dielectric constant ε_f . The dielectric function of the nonlinear dielectric cover is assumed to be Kerr-like and isotropic, it depends on the electric field and can be written as for TE waves, $e^{NL} = e_2 + aE_y^2$, where the ε_2

is the linear part of the dielectric function and α the nonlinearity coefficient. The conventional magnetostatic potential Ψ from Maxwell's equation [14],

$$H = \nabla\Psi \tag{1.2a}$$

$$\Psi = A\sinh(kz)\exp[i(kx - 2pft)] \tag{1.2b}$$

For the TE magnetostatic waves in a YIG can be written as:

$$h_x^{(1)} = ik\Psi \tag{1.2c}$$

$$h_z^{(1)} = -ikA\cosh(kz)\exp[i(kx - 2pft)] \tag{1.2d}$$

$$e_y^{(1)} = \frac{2pfm_0}{k}\left(-m_{xz}h_x + m_{xx}h_z\right) \tag{1.2e}$$

The field components of the wave in the nonlinear cover can be obtained:

$$E_y^{(2)}(z) = \frac{1}{k_0}\left(\frac{2}{a}\right)^{1/2}\frac{k_2}{\cosh[k_2(z - z_0)]} \tag{1.3a}$$

Where $k_0 = 2\pi f / c$ and z_0 is a constant to be determined from the boundary conditions, and:

$$h_x^{(2)}(z) = -\frac{k_2}{2pfm_0}\tanh[k_2(z - z_0)]E_y^{(2)}(z) \tag{1.3b}$$

$$h_z^{(2)}(z) = -\frac{k}{2pfm_0}E_y^{(2)}(z) \tag{1.3c}$$

Applying the boundary conditions, the complete dispersion equation is found to be:

$$\tanh(k_2 z_0) = \left(\frac{-m_{xx}\coth kd + Sm_{xz}}{m_{xx}m_v}\right) \tag{1.4a}$$

Where $m_v = \left(m_{xx}^2 - m_{xz}^2\right)/m_{xx}, S = \pm 1, S = 1$ stands for the propagation of the waves in forward direction, and $S = -1$ for the propagation of the waves in backward direction. In terms of the interface nonlinearity, the dispersion equation is written as:

$$\frac{a}{2}E_y^2(d)=1-\left(\frac{-m_{xx}\coth kd+Sm_{xz}}{m_{xx}m_v}\right) \tag{1.4b}$$

Where $(a/2)E_y^2(d)$ is the interface nonlinearity at $z = d$. In the linear limit, we get [14]:

$$e^{-2kd}=\frac{[1+(m_{xx}-Sm_{xz})][1+(m_{xx}+Sm_{xz})]}{[1-(m_{xx}+Sm_{xz})][1-(m_{xx}-Sm_{xz})]} \tag{1.4c}$$

The dispersion relation or the propagation characteristics are shown in Fig.(1.1) for different values of the film thickness. All of the dispersion curves shift to the left rapidly for higher values of the film thickness in both directions and after a while shift to the right for the backward wave direction. The fast shift is due to the effect of the nonlinearity of the cover, which did not happen in the linear case.

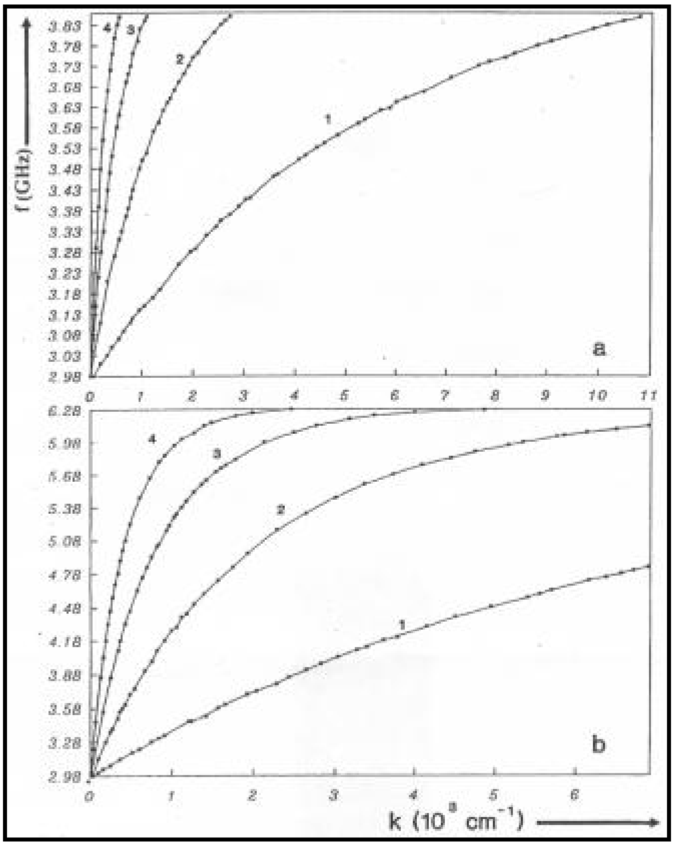

Fig. (1.1): Computed dispersion case in a) forward and b) backward wave direction at $(a/2)E_y^2(d)=0.6$, $m_0H_0=0.05$ T, $m_B=1.25$, $m_0M_0=0.1750$ T, $e_f=1, e_2=2.25$, $g=1.76\times10^{11}$ rad s^{-1} T^{-1} , (1) $d =$ 0.5, (2) 2, (3) 5, and (4) 10 µm

1.4 Nonlinear magnetostatic surface waves in a gyromagnetic film

The purpose is to report in detail the approach and the results of a new type of strongly nonlinear magnetostatic surface wave in a YIG film, bounded by a nonlinear cover and a dielectric substrate [13]. The numerical results for the strongly nonlinear magnetostatic surface waves in a YIG film are also presented and discussed, especially the dispersion characteristics and the difference between the phase constants of the wave propagation in the two directions. It has been shown that the non-reciprocity can be minimized for smaller operating frequencies and relatively thick films. These calculations might be useful and important for accurate modeling of future magnetostatic surface wave device performance.

The geometry and coordinate system used is as shown in Fig.(1.2), and the magnetic permeability tensor of the gyromagnetic ferrite (YIG) substrate is as described before. The ferrite has also a dielectric constant ε_f. The dielectric function of the nonlinear dielectric cover is assumed to be Kerr-like and isotropic, it depends on the electric field and can be written as for TE waves, $e^{NL} = e_3 + aE_y^2$, where the ε_3 is the linear part of the dielectric function and α is the nonlinear coefficient.

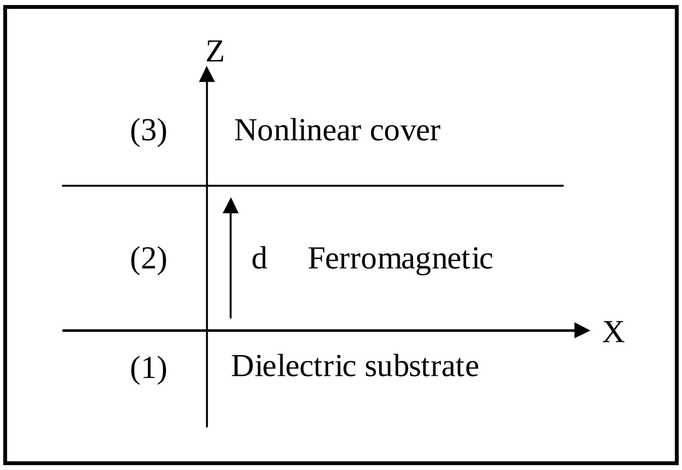

Fig. (1.2): Coordinate system for a ferrite (YIG) film bounded by a nonlinear cover and a dielectric substrate, the applied magnetic field is in the y-axis.

The important restrictions and assumptions made in the analysis are listed below [13]:

(1) The magnetostatic approximation $\overline{\nabla} \times \overline{H} = 0$ is employed in the gyromagnetic and substrate media, and the magnetostatic range is imposed where $k \geq w/c$.

(2) Nonlinear effect in the gyromagnetic film is neglected compared with the dominant nonlinear effects in the cover medium.

(3) The magnetostatic approximation $\overline{\nabla} \times \overline{H} = 0$ is not employed in the nonlinear medium, because the electric field in Maxwell's equations cannot be ignored and therefore the magnetostatic approximation is not valid, but the magnetostatic range can be applied.

We seek solution of Maxwell's equations for the TE (s-polarized) waves in the three layers taking into account the above restrictions and assumptions.

In a linear dielectric substrate, Ψ can be written as:

$$\Psi^{(1)} = a_1 \exp(kz) \exp[i(kx - 2pft)] \tag{1.5a}$$

Where a_1 is an amplitude coefficient determined from the boundary condition

$$h_x^{(1)} = ik\Psi^{(1)} \tag{1.5b}$$

$$h_z^{(1)} = ik\Psi^{(1)} \tag{1.5c}$$

$$e_y^{(1)} = \frac{wm_0}{k} h_z^{(1)} \tag{1.5d}$$

and in the yttrium iron garnet film,

$$\Psi^{(2)} = [a_2 \exp(kz) + b_2 \exp(-kz)] \exp[i(kx - 2pft)] \tag{1.6a}$$

$$h_x^{(2)} = ik\Psi^{(2)} \tag{1.6b}$$

$$h_z^{(2)} = -ik[a_2 \exp(kz) - b_2 \exp(-kz)] \exp[i(kx - 2pft)] \tag{1.6c}$$

$$e_y^{(2)} = \frac{wm_0}{k} \left(-m_{xz} h_x^{(2)} + m_{xx} h_z^{(2)}\right) \tag{1.6d}$$

Where a_2 and b_2 are amplitude coefficients determined from boundary conditions. From Maxwell's equations for the nonlinear dielectric cover, we get:

$$-\frac{\partial}{\partial z}E_y = iwm_0H_0 \tag{1.7a}$$

$$kE_y = -wm_0H_z \tag{1.7b}$$

$$-ikH_z + \frac{\partial}{\partial z}H_x = -iwe_0e^{NL}E_y \tag{1.7c}$$

Eliminating H_x and H_z from Eq's.(1.7a) and (1.7b) and using Eq.(1.7c) give the result:

$$\frac{\partial^2}{\partial z^2}E_y(z) - \left(k^2 - k_0^2 e_3\right)E_y(z) + k_0^2 a E_y^3(z) = 0 \tag{1.8a}$$

Consider the wave vector in the magnetostatic range as $k \geq (w/c)e_3^{1/2}$; so

$$\frac{\partial^2 E_y(z)}{\partial z^2} - k^2 E_y(z) + \frac{w^2}{c^2} a E_y^3(z) = 0 \tag{1.8b}$$

The solution of the wave equations (1.8b), which falls to zero as z goes to infinity

$$E_y^{(3)}(z) = \frac{1}{k_0}\left(\frac{2}{a}\right)^{1/2} \frac{k}{\cosh[k(z - z_0)]} \tag{1.8c}$$

$$h_x^{(3)}(z) = -\frac{k}{wm_0}\tanh[k(z - z_0)]E_y^{(3)}(z) \tag{1.8d}$$

$$h_z^3(z) = \frac{k}{wm_0}E_y^{(3)}(z) \tag{1.8e}$$

Applying the boundary conditions, the complete dispersion equation is found to be [13]:

$$\exp(-2kd) = \frac{[1 + u(m_{xx} - Sm_{xz})][1 + (m_{xx} + Sm_{xz})]}{[1 - u(m_{xx} + Sm_{xz})][1 - (m_{xx} - Sm_{xz})]} \tag{1.9a}$$

Where $u = \tanh[k(d - z_0)]$ varies from zero to unity, according to the values of the cover-film interface nonlinearity. Noting that the reversal of the sign of μ_{xz} changes the dispersion relation, this implies that the dispersion relation of the nonlinear magnetostatic surface waves exhibits the non-reciprocity phenomenon.

In the linear limit u = 1 or α = 0, we get the dispersion equation

$$\exp(-2kd) = \frac{[1+u(m_{xx}-Sm_{xz})][1+(m_{xx}+Sm_{xz})]}{[1-(m_{xx}+Sm_{xz})][1-(m_{xx}-Sm_{xz})]} \qquad (1.9b)$$

This is the dispersion equation for magnetostatic surface waves in a single ferrite (YIG) film derived by Damon and Eshbach (1961) and Sodha and Srivastava (1981), as mentioned in [13].

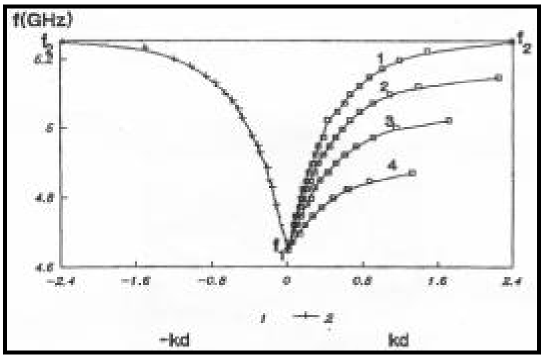

Fig. (1.3): Computed dispersion curves for several values of the nonlinear term u (d = 1 cm; $\mu_0 H_0$ = 0.1 T; μ_B = 1; $\mu_0 M_0$ = 0.1750 T; ε_f = 1; γ = 2.7 MHz Oe^{-1}): curve 1, u = 1; curve 2, $u = (0.9)^{1/2}$; curve 3, $u = (0.7)^{1/2}$; curve 4, $u = (0.5)^{1/2}$.

The propagation characteristics of strongly nonlinear magnetostatic guided by a YIG film is computed by solving eq.(1.9a) for different values of the nonlinear terms u shown in Fig.(1.3). Curve (1) represents the linear dispersion relation of the magnetostatic surface waves, as the linear terms equals unity.

The differential phase constant or the phase shift $\Delta\beta$ between the counter-propagation waves is calculated from eq.(1.9a) as[13]:

$$b_{\pm} = \frac{1}{2dk_0}\ln\left(\frac{[1+u(m_{xx}-Sm_{xz})][1+(m_{xx}-Sm_{xz})]}{[1-u(m_{xx}-Sm_{xz})][1-(m_{xx}-Sm_{xz})]}\right) \qquad (1.9c)$$

Where $b_{\pm} = k_{\pm}/k_0$ and $\Delta b = b_{-} - b_{+}$

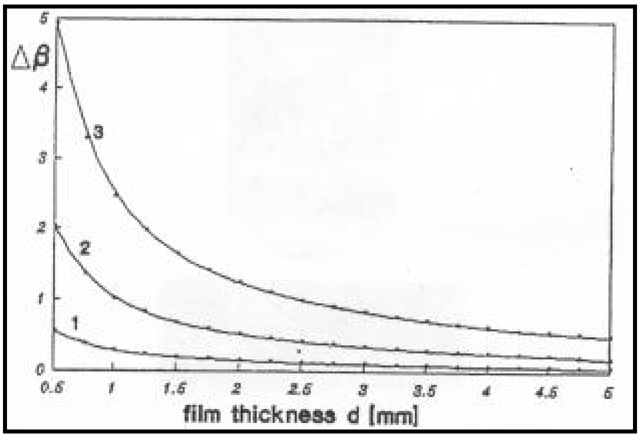

Fig. (1.4): Computed difference between the phase constants for wave propagation in the two directions (u = 0.7; d = 1 cm; μ_B = 1; $\mu_0 H_0$ = 0.1 T; $\mu_0 M_0$ = 0.1750 T; ε_f = 1; γ = 2.7 MHz Oe^{-1}): curve 1, f = 4.7 GHz; curve 2, f = 4.8 GHz; curve 3, f = 4.9 GHz.

Fig. (1.4) shows the differential phase constant or the phase shift $\Delta\beta$ of the wave propagation in the positive and negative x-directions (forward and backward) against the film thickness of the YIG film for different values of signal operating frequency.

1.5 Conclusions

For $m_v \leq 0$ which is the region of interest, the frequency lies within the range from $\sqrt{f_0(f_0+f_m)}$ to f_0+f_m. The dispersion curve in the forward wave direction originates at the point $f_1=\sqrt{f_0(f_0+f_m)}$ and terminates at $f_2=f_0+f_m/2$. While the dispersion curve in the backward wave direction originates at f_1 and terminates at $f_3 = f_0 + f_m$, where f_1 , f_2 and f_3 have the same values as for the linear propagation characteristics of the waves.

All of the dispersion curves [14] shift to the left rapidly for higher values of the film thickness in both directions and after a while shift to the right for the backward wave direction. The fast shift is due to the effect of the nonlinearity of the cover, which did not happen in the linear case. Both figures (1.3) and (1.4) show the nonreciprocal behavior, which is very important if one wants to design microwave devices as isolators, switches, and oscillators or for use in microwave signal processing technology.

It is shown [13] that the three-layer structure exhibits minimum non-reciprocity in the propagation constant that is $\Delta\beta$ becomes a minimum, when the structure has thicker film and a smaller operating frequency, especially near the resonance frequency f_1 . This means that the value of the non-reciprocity can be tuned and controlled by adjusting the signal operating frequency and the YIG film thickness.

1.6 Development of (LHM's)

Left-handed materials (**LHM's**) with negative both magnetic permeability (μ) and dielectric permittivity (ε) have recently attracted a great deal of attention because of their promise for its applications in different fields. So, these materials have a negative refractive index, which implies that the phase and group velocities of the propagating electromagnetic wave oppose each other.

This property of these **LHM's** is responsible for their anomalous physical behavior. Since materials with negative refractive index do not naturally occurs, they have to be artificially constructed in the form of metal rods and split-ring resonators [3].

Theoretical studies on electrodynamics of media with negative permittivity (ε) and negative permeability (μ) are back to the 1940s – 1960s.

The spin-wave modes of magnetized thin film also analyzed by Damon and Eshbach in 1961 [12], where a tangentially-magnetized film is known to exhibit backward wave behavior within a range of angles around the direction of the bias field.

Earlier in 2000, Shelby et al. [4] announced that they had developed a left-handed material for the first time, using the array of wires and split-ring resonator as described by Veselago [1]. That is a beam incident on a left-handed material (LHM) from an ordinary right-handed medium (RHM) was shown to refract to the same side of the normal as the incident beam.

Pendry predicted [5], at radio frequencies, an array of parallel wires would behave like a material with negative permittivity (ε), and an array of C-shaped circuits known as split-ring resonators would behave like a material with negative permeability. By constructing an array consisting of both wires and split-ring resonators, the group created a "material" with negative (μ,ε) at frequencies around 10 GHz.

1.6.1 What is LHM's?

In general, materials have two parameters, permeability (μ) and permittivity (ε) that determine how the material will interact with electromagnetic radiation, which includes light, microwaves, radio waves, even x-ray. A Left-Handed material is a material whose permeability and permittivity are simultaneously negative ($\varepsilon < 0$, $\mu < 0$), (i.e., $E\times H$ lies along the direction of $-k$ for propagating plane waves) [3].

The general form of the negative effective permeability, μ_{eff} (ω) and effective permittivity ε_{eff} (ω) has been studied by Pendry et al. [6-7] and described as:

$$m_{eff}(w) = 1 - \frac{Fw^2}{w^2 - w_0^2 + iw\Gamma} \tag{1.10a}$$

Where, ω_0 is the resonance frequency, Γ is the damping parameter and F is constant.

And $$e_{eff}(w) = 1 - \frac{w_p^2 - w_0^2}{w^2 - w_0^2 + iw\Gamma} \tag{1.10b}$$

Where, ω_p is the plasma frequency, ω_0 is the resonance frequency and Γ is the damping parameter.

More evidently, it has been found in LHM's the wave vector of a monochromatic plane wave is reversed in comparison with what it should have been for RHM. That means that if the vector *E* is along x-axis and the vector *B* is along y-axis, in the RHM the electromagnetic wave will propagate along z-axis, while in LHM the wave propagate along – z-axis. Figs. (1.5a, 1.5b) respectively show this propagation.

In addition, index of refraction n being negative tells that the direction of energy propagation is opposite to the direction of plane wave motion.

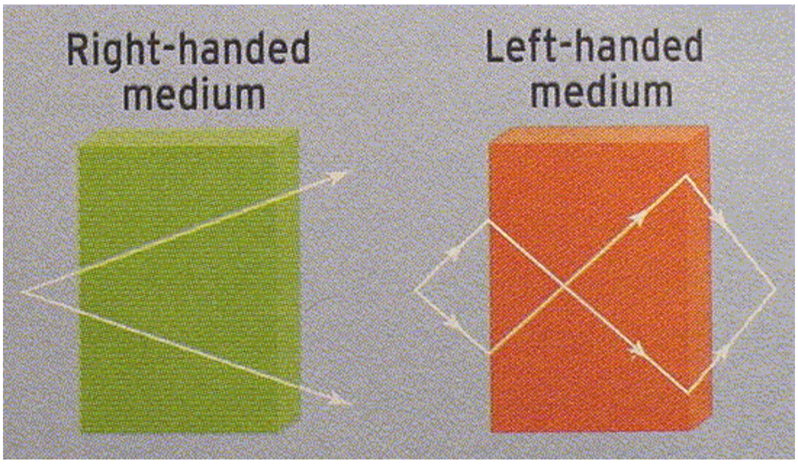

Fig. (1.5a)

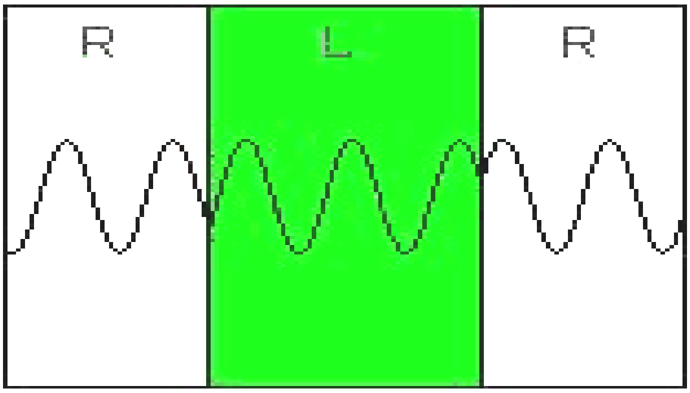

Fig. (1.5 b)

Figs. (1.5a), (1.5b): shows the propagation of wave vector along RHM's and LHM's respectively

1.6.2 Fabrication of LHM's

Until now the theoretists did not find a natural material characterized by negative permeability (μ) and negative permittivity (ε), but these materials are fabricated [2], and named artificial materials.

For example, photonic crystals and metamaterials are currently being investigated for such left handedness of EM wave, while a few other artificial materials are feasible.

I) Photonic crystal

Photonic crystal is an array of either dielectric or metallic rods or holes in a dielectric medium. The photonic crystal can be designed to possess left-handed behavior in a chosen frequency of interest, for example optical to microwave frequencies. Fig. (1.5c) show the formation of fabricated photonic crystal.

Fig. (1.5 c): shows the fabricated photonic crystal.

II) Metamaterials

This material was fabricated by interleaving split ring resonator (SRR) and metallic wire strips (WS) [3-4]. Using lithography techniques to produce arrays of split ring resonators (SRR) on one side and wire strips (WS) on the other side should result in an effective negative permeability and negative permittivity material. This material has negative index. Fig. (1.5d) show the picture of fabricated of metamaterial.

Fig. (1.5 d): shows the fabricated metamaterial.(SRR)

1.6.3 Application of LHM's

Every one believes that when one creates a new material that scatters electromagnetic radiation in a unique manner, some useful purpose will be found. For example, uses in the cellar communications industry, where novel filters, antennas, and other electromagnetic devices are of great importance.

1.7 M.S.S.W's and LHM's

In this thesis, we investigate the properties of the dispersion of nonlinear magnetostatic surface waves between two media, one of which is left-handed (LHM) with both ($\mu < 0$, $\varepsilon < 0$) and the other is a gyromagnetic (ferrite) medium. We investigate theoretically the behavior of magnetostatic surface waves on left-handed materials. We derive the dispersion equation and solve it numerically.

Finally, we hope the obtained results could be used in future work in opto-microwaves technology.

2.1 Introduction

In this chapter we give a survey to the work of R. F. Wallis [23] on semi-infinite magnetic media, since he considered the surface polaritons as TE-modes. We follow his mathematical approach and derive all the obtained dispersion relations. We make a numerical computation in order to calculate the propagation characteristic of the nonlinear dispersion equation. Also we discuss the case of surface polaritons on ferromagnetic metals, which have a dielectric tensor function of the general form of equation (2.40). The first-layer structure exhibits the non-reciprocity, while the other is not.

2.2 Case one: vacuum / ferrite media

2.2.1 Theory and dispersion relations

Fig. (2.1) shows the coordinate system used. We assume that the space above the medium to be vacuum ($\varepsilon_0 = \mu_0 = 1$) and a semi-infinite medium characterized by a gyromagnetic permeability tensor as a ferrite (YIG).

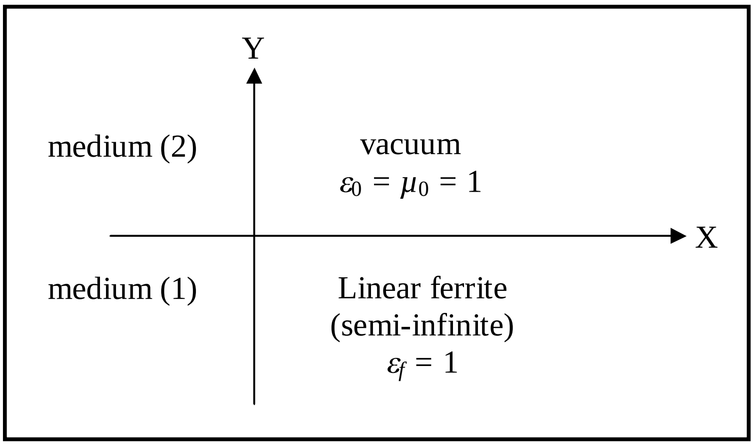

Fig. (2.1): Coordinate system for a single interface between a vacuum and a linear ferromagnetic.

Only TE-modes are going to be considered and propagate along x-axis with wave number (K) and angular frequency ω. The gyromagnetic ferrite substrate in this case has magnetic permeability tensor as:

$$m(w)=\begin{pmatrix} m_{xx} & m_{xy} & 0 \\ m_{yx} & m_{yy} & 0 \\ 0 & 0 & m_{zz} \end{pmatrix} \qquad (2.1)$$

We consider a single domain ferromagnetic insulator magnetized along $+\hat{z}$ axis by an external static magnetic field H_0. So, this field may be zero and we take μ_{xx} and μ_{zz} to be real, and μ_{xy} to be pure imaginary. Also, we take $\mu_v(\omega)$, the Voigt configuration magnetic permeability function given by:

$$m_v(w)=m_{xx}+\frac{m_{xy}^2}{m_{xx}} \qquad (2.1a)$$

2.2.2 The electric and magnetic field components

I) For the vacuum cover: medium 2

In this case, Maxwell's equations lead to a wave equation and divergence equation as shown:

$$\nabla^2 H-\nabla\nabla.H-\frac{m}{c^2}\ddot{H}=0 \qquad (2.2)$$

$$\nabla.mH=0 \qquad (2.3)$$

Now, we can consider that the surface polariton will be a TE mode with $E \,//\, \hat{z}$ (Hz = 0) and attenuating exponentially away from the surface.

$$H=H_0\exp(ikx)\exp(-a_0 y)\exp(-iwt) \qquad y>0 \qquad (2.4)$$

$$H=H_1\exp(ikx)\exp(a_1 y)\exp(-iwt) \qquad y<0 \qquad (2.5)$$

Where ω, k, α_0, α_1 are all constrained to be real, and the subscripts 0 and 1 refer to the vacuum and medium respectively.

Substituting Eq. (2.4) in Eq. (2.2), we get:

$$\left(\frac{\partial^2}{\partial x^2}+\frac{\partial^2}{\partial y^2}+\frac{\partial^2}{\partial z^2}\right)H-\nabla\nabla.H-\frac{m}{c^2}\frac{\partial^2}{\partial t^2}H=0 \qquad (2.6)$$

$$\nabla\nabla.H=0 \qquad (2.7)$$

$$\left(-k^2+a_0^2\right)H+\frac{m_0 w^2}{c^2}H=0 \qquad (2.8)$$

Where, μ_0 for vacuum = 1, then:

$$\left(-k^2 + a_0^2 + \frac{w^2}{c^2}\right)H = 0 \tag{2.9}$$

Which this leads to the first dispersion relation,

$$\frac{w^2}{c^2} - k^2 + a_0^2 = 0 \tag{2.10}$$

II) For the ferrite substrate: medium 1

The ferrite has a permeability tensor as shown in Eq's. (2.1) and (2.1a).

Using Maxwell's equation we get:

$$\nabla \times E = iwm_0 m(w)H \tag{2.11}$$

$$\nabla \times H = -iwe_0 e_f(w)E \tag{2.12}$$

From Eq. (2.11), we have:

$$\begin{vmatrix} \hat{i} & \hat{j} & \hat{k} \\ ik & \dfrac{\partial}{\partial y} & 0 \\ 0 & 0 & E_z \end{vmatrix} = iwm_0 \begin{pmatrix} m_{xx} & m_{xy} & 0 \\ -m_{xy} & m_{yy} & 0 \\ 0 & 0 & m_{zz} \end{pmatrix} \begin{pmatrix} H_x \\ H_y \\ 0 \end{pmatrix} \tag{2.13}$$

Then the electric and magnetic field components,

$$\frac{\partial E_z}{\partial y} = iwm_0\left(m_{xx}H_x + m_{xy}H_y\right) \tag{2.14}$$

$$-ikE_z = iwm_0\left(-m_{xy}H_x + m_{xx}H_y\right) \tag{2.15}$$

Similarly, from Eq. (2.12), we have:

$$\begin{vmatrix} \hat{i} & \hat{j} & \hat{k} \\ ik & \dfrac{\partial}{\partial y} & 0 \\ H_x & H_y & 0 \end{vmatrix} = -\hat{i}we_o e_f \begin{pmatrix} 0 \\ 0 \\ E_z \end{pmatrix} \tag{2.16}$$

Then,

$$ikH_y - \frac{\partial H_x}{\partial y} = -iwe_0 e_f E_z \tag{2.17}$$

Multiplying Eq. (2.14) by μ_{xx} and Eq. (2.15) by μ_{xz}, then Eq. (2.14) and Eq. (2.15) become:

$$m_{xx}\frac{\partial E_z}{\partial y} = iwm_0\left(m_{xx}^2 H_x + m_{xx} H_{xy} H_y\right) \tag{2.18}$$

$$ikm_{xy}E_z = iwm_0\left(m_{xy}^2 H_x + m_{xx} H_{xy} H_y\right) \tag{2.19}$$

By adding Eq. (2.18) and Eq. (2.19), we get:

$$m_{xx}\frac{\partial E_z}{\partial y} + ikm_{xy}E_z = iwm_0\left(m_{xx}^2 + m_{xy}^2\right)H_x \tag{2.20}$$

Then we have:

$$\frac{\partial E_z}{\partial y} + ik\frac{m_{xy}}{m_{xx}}E_z = iwm_0 m_v H_x \tag{2.21}$$

Where, $m_v = \left(m_{xx}^2 + m_{xy}^2\right)\big/ m_{xx}$ (2.21a)

In the same way, multiplying Eq. (2.14) by μ_{xz} and Eq. (2.15) by $(-m_{xx})$, we get,

$$m_{xy}\frac{\partial E_z}{\partial y} = iwm_0\left(m_{xx}m_{xy}H_x + m_{xy}^2 H_y\right) \tag{2.22}$$

$$-ikm_{xx}E_z = iwm_0\left(-m_{xx}m_{xy}H_x + m_{xx}^2 H_y\right) \tag{2.23}$$

By adding Eq. (2.22) to Eq. (2.23), we get:

$$m_{xy}\frac{\partial E_z}{\partial y} - ikm_{xx}E_z = iwm_0\left(m_{xx}^2 + m_{xy}^2\right)H_y$$

dividing

(2.24)

By both sides by μ_{xx}, we obtain:

$$\frac{m_{xy}}{m_{xx}}\frac{\partial E_z}{\partial y} - ikE_z = iwm_0 m_v H_y$$

(2.25)

Where, $m_v = \left(m_{xx}^2 + m_{xy}^2\right)\big/ m_{xx}$ (2.25a)

Differentiate Eq. (2.21) with respect to *y* gives,

$$\frac{\partial^2 E_y}{\partial y^2} + ik\frac{m_{xy}}{m_{xx}}\frac{\partial E_z}{\partial y} = iwm_0 m_v \frac{\partial H_x}{\partial y} \tag{2.26}$$

But from Eq. (2.17) and Eq. (2.25), we have respectively,

$$\frac{\partial H_x}{\partial y} = ikH_y + iwe_0 e_f E_z \tag{2.27}$$

$$\frac{\partial E_y}{\partial y} = ik \frac{m_{xx}}{m_{xy}} E_z + iwm_0 m_v \frac{m_{xx}}{m_{xy}} H_y \tag{2.28}$$

Substitute both Eq's. (2.27) and (2.28) in Eq. (2.26), we obtain:

$$\frac{\partial^2 E_y}{\partial y^2} + ik \frac{m_{xy}}{m_{xx}} \left(ik \frac{m_{xx}}{m_{xy}} E_z + iwm_0 m_v \frac{H_{xx}}{m_{xy}} H_y \right) = iwm_0 m_v \left(ikH_y + iwe_0 e_f E_z \right) \tag{2.29}$$

$$\frac{\partial^2 E_z}{\partial y^2} - k^2 E_z - kwm_0 m_v H_y = -wm_0 m_v kH_y - w^2 m_0 m_v e_0 e_f E_z$$

$$\frac{\partial^2 E_z}{\partial y^2} - k^2 E_z + w^2 m_0 m_v e_0 e_f E_z = 0 \tag{2.30}$$

$$\frac{\partial^2 E_z}{\partial y^2} - \left(k^2 - w^2 m_0 e_0 m_v e_f \right) E_z = 0 \tag{2.31}$$

Let $\frac{1}{c^2} = m_0 e_0$ and $\varepsilon_f = 1$ (2.31a)

Substitute Eq. (2.31a) in Eq. (2.31), we get:

$$\frac{\partial^2 E_z}{\partial y^2} - \left(k^2 - \frac{w^2}{c^2} m_v \right) E_z = 0 \tag{2.32}$$

Let $a_1^2 = k^2 - \frac{w^2}{c^2} m_v$ (2.32a)

With $m_v = \left(m_{xx}^2 + m_{xy}^2 \right) / m_{xx}$ (2.32b)

Finally, we get on the differential equation in terms of E_z,

$$\frac{\partial^2 E_z}{\partial y^2} + a_1^2 E_z = 0 \tag{2.33}$$

The solutions of Eq. (2.33) for the field components $H_x(y)$, $H_y(y)$, $E_z(y)$ are:

$$E_z = E_0 e^{-a_1 y} \tag{2.34}$$

$$H_x(y) = \left(\frac{-k_1 m_{xx} + ikm_{xy}}{iwm_0 m_{xx} m_v} \right) E_z \tag{2.35}$$

$$H_y(y) = -\left(\frac{k_1 m_{xy} + ikm_{xx}}{iwm_0 m_{xx} m_v}\right)E_z \tag{2.36}$$

Where E_0 is the total electrical field in region (1).

From equation (2.32a), we can get the second dispersion relation,

$$\frac{w^2}{c^2} m_v - k^2 + a_1^2 = 0 \tag{2.37}$$

Where, $m_v = m_{xx} + m_{xy}^2 / m_{xx}$ is the permeability for propagation in the Voigt configuration.

Substitute both Eq's. (2.4) and (2.5) into Eq. (2.3), and applying the normal boundary conditions on *B* and *H* and solving simultaneously, we obtain a relationship between α_0 and α_1 which is named the third dispersion relation as:

$$a_1 = -a_0 m_v - ik\frac{m_{xy}}{m_{xx}} \tag{2.38}$$

Finally, by solving both Eq's. (2.10), (2.37), and (2.38) simultaneously, we end up with the complete dispersion relation:

$$\frac{k^2 c^2}{w^2} = \left(\frac{(m_v - 1)(m_{xx} m_v - 1)m_{xx} + 2m_{xy}^2 \pm 2im_{xy}\left[(m_{xx} - m_{xx} m_v - 1)\right]^{1/2}}{(m_{xx} m_v - 1)^2 + 4m_{xy}^2}\right) \tag{2.39}$$

In general, Eq. (2.39) has two physical solutions for ω(k). The first solution shows the nonreciprocal propagation as shown in Fig. (2.3) and the other is unexpected, because there is no propagation in its case.

2.3 Case two: surface polaritons on ferromagnetic metals

In case one, we have treated the case where gyrodielectric medium ε(ω) = 1. But in the second case we consider the dielectric tensor function of the general form, such ferromagnetic metal as:

$$e(w) = \begin{pmatrix} e_{xx} & e_{xy} & 0 \\ e_{yx} & e_{yy} & 0 \\ 0 & 0 & e_{zz} \end{pmatrix} \tag{2.40}$$

Since, for isotropic medium the only component of ε(ω) which enters into the magnetic dipole surface polariton in Fig. (2.1) is ε_{zz} [23].

In particular, we consider the surface polariton is TE mode as in Eq's. (2.4) and (2.5) of the case one, with $E \,//\, \hat{z}$ and therefore only ε_{zz} component couples to E. We follows our analysis such as in the previous treatment (case one), then we get anomalous dispersion relations like Eq. (2.37).

$$\frac{w^2}{c^2} m_v e_{zz} - k^2 + a_1^2 = 0 \qquad (2.41)$$

Hence, we get the complete surface polariton dispersion relation which is given by:

$$\frac{k^2c^2}{w^2} = \left(\frac{(m_v - e_{zz})(m_{xx}m_v - 1)m_{xx} + 2m_{xy}^2 \pm 2im_{xy}\left[m_{xx}\left\{e_{zz}^2 m_{xx} - e_{zz}(m_{xx}m_v - 1) + m_{xx}\right\}\right]^{1/2}}{(m_{xx}m_v - 1)^2 + 4m_{xy}^2} \right) \qquad (2.42)$$

With $e_{zz}(w) = e_0\left(1 - \frac{w_p^2}{w^2}\right)$ (2.41a)

Where ω_p is the screened plasma frequency, ε_0 is the high frequency electric dipole excitations, and:

$$w_p = \left(\frac{4pne^2}{m^* e_0}\right)^{1/2} \qquad (2.42b)$$

Where m^* denotes the effective mass of electron.

Finally, we notice that Eq. (2.42) is similar to Eq. (2.39) but the difference is the presence of ε_{zz}, ε_{xx}, ε_v instead of μ_{zz}, μ_{xy}, μ_v respectively.

Wallis [23] said that the bulk propagation in the case of ferromagnetic metals does not occur when $\varepsilon_{zz}(\omega)$ and $\mu(\omega)$ are both positive, while when $\varepsilon_{zz}(\omega)$ and $\mu_v(\omega)$ are both negative the propagation occurs under appropriate parameters for a ferromagnetic metal.

Furthermore, the general electrodynamics of bulk polaritons in a medium with simultaneously negative values of ε (ω) and μ(ω) will be discuss in the next chapter as discussed by Veselago (1968) [1-12].

2.4 Conclusions

A complete dispersion relation is derived [Eq. (2.39)] in the case one between a surface polaritons on a semi-infinite medium, where only one boundary (ferrite / vacuum) and another anomalous dispersion equation is derived also [Eq. (2.42)] between ferromagnetic metal and vacuum.

After numerical analysis using software program [24], and for $m_v \leq 0$, which is the region of interest as in Fig. (2.2), where the frequency lies within the range 3.5 GHz and 5.5 GHz. The dispersion curves (a) forward, (b) backward in Fig. (2.3) which are the relation between the frequency *f* (Hz) and the wave vector *k* (m^{-1}). Also, Fig. (2.3) shows both wave propagation backward and forward for $S = \pm 1$ respectively. This propagation represents the nonreciprocal behavior.

While in case two the non-reciprocity does not occur between ferromagnetic metal and vacuum [23].

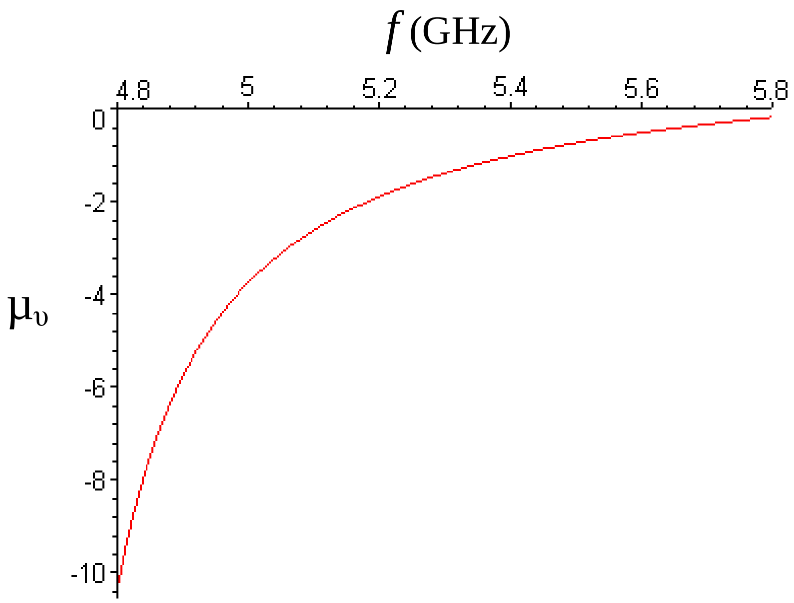

Fig. (2.2): shows the effective permeability μ_υ as a function of frequency f. $\mu_0 H_0 = 0.05$ T, $\mu_B = 1.25$, $\mu_0 M_0 = 0.1750$ T, $\gamma = 1.76 \times 10^{11}$ rad s^{-1} T^{-1}

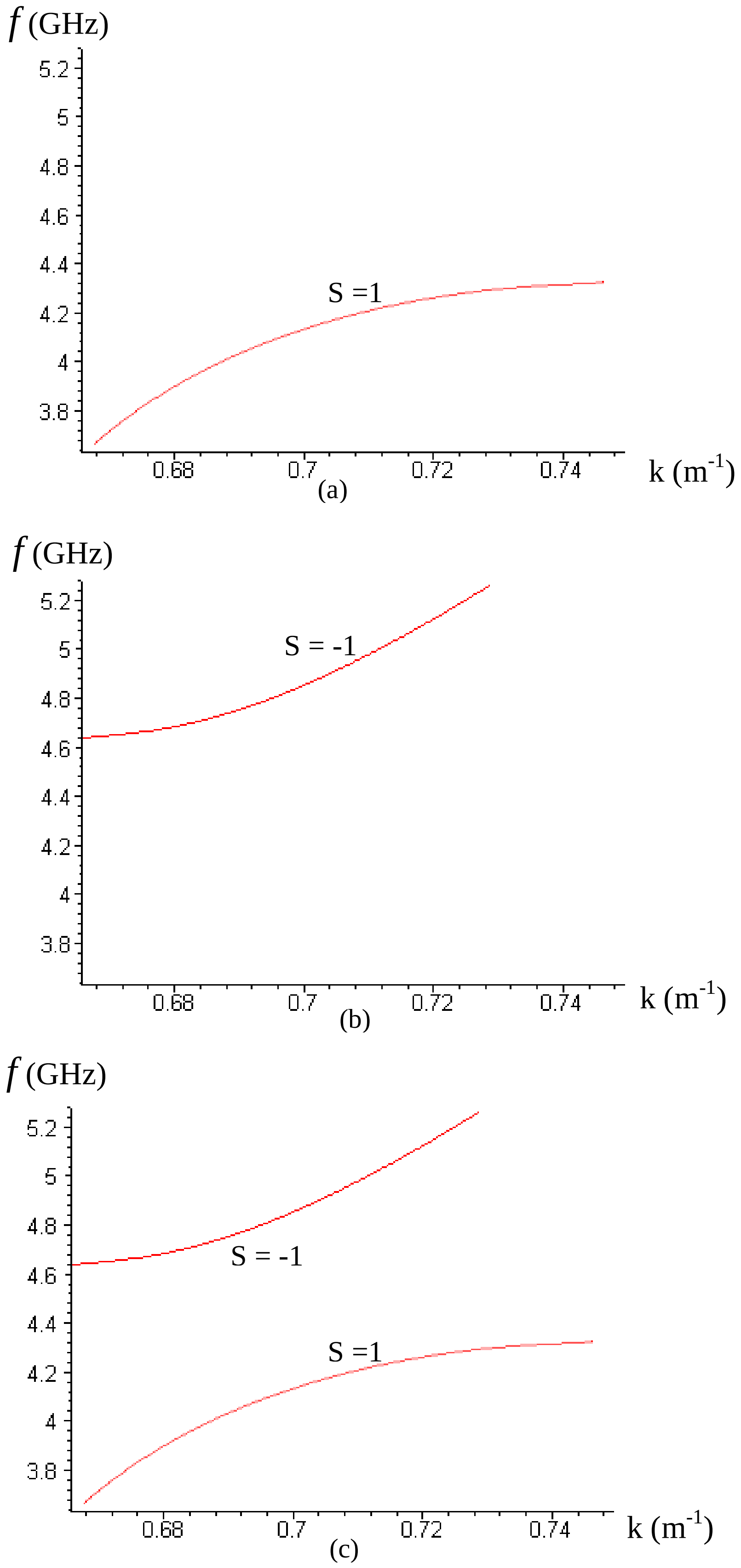

Fig. (2.3): shows the computed dispersion curves in (a) forward, (b) backward and (c) both wave propagation. $\mu_0H_0 = 0.5$ T, $\mu_B = 1.25$, $\mu_0M_0 = 0.1750$ T, $\gamma = 1.76 \times 10^{11}$ rad s^{-1} T^{-1}

3.1 Introduction

The nonlinear magnetostatic surface waves that propagate along the planner interfaces between different media, in cases where at least one of the media is LHM, have attracted much attention in recent years [8]. The general theory for two media has been investigated [23], and the dispersion relation is derived and analyzed numerically between ferrite-vacuum media. In this chapter, we derive a new-exact analytical dispersion relation of magnetostatic surface waves. These waves are considered to propagate in layered structure containing a semi-infinite linear (ferrite substrate) and a left handed material.

The left handed material characterized by [7]:

$$m_{eff}(w) = 1 - \frac{Fw^2}{w^2 - w_0^2} \quad , \quad e_{eff}(w) = 1 - \frac{w_{ep}^2}{w^2} \tag{3.1}$$

Where $F = 0.56$, $\omega_0 / 2\pi = 4$ GHz , and $\omega_{ep} / 2\pi = 10$ GHz

3.2 Theory and dispersion relations

The guiding structure that considered consists of a linear semi-infinite ferrite substrate assumed to be YIG, and a left-handed material with $\varepsilon < 0$, $\mu < 0$ cladding in constant everywhere on the z = 0 plane. We consider TE s-polarized waves that propagate in the x-direction with wave number k and angular frequency ω. The applied magnetic field is normal to the wave propagation and the z-axis is perpendicular to the plan separating the structure layers as shown in Fig. (3.1).

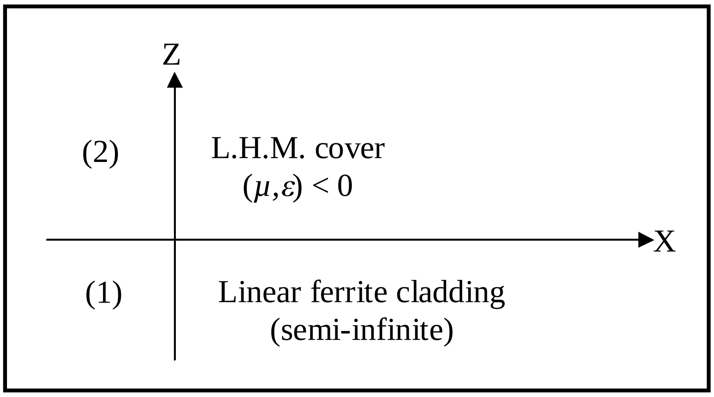

Fig. (3.1): Coordinate system for the single interface between LHM and a linear ferrite cladding, the applied magnetic field is in the Y-direction.

3.2.1 For the ferrite substrate

The magnetostatic potential Ψ of the magnetostatic surface waves in the YIG film is written [8] as:

$$\Psi^{(1)} = A\exp(kx)e^{i(kx-wt)} \tag{3.2}$$

The relevant component of the magnetic fields for the TE magnetostatic waves in the YIG can be written after considering the phase difference as:

$$h_x^{(1)} = ikA\exp(kz)e^{i(kx-wt)} \tag{3.2a}$$

$$h_z^{(1)} = -ikA\exp(kz)e^{i(kx-wt)} \tag{3.2b}$$

$$e_y^{(1)} = \frac{wm_0}{k}\left(-Sm_{xz}h_x^{(1)} + m_{xx}h_z^{(1)}\right) \tag{3.2c}$$

Where $S = \pm 1$, S = 1 stands for the propagation of the waves in forward direction, and S = -1 for the backward direction.

3.2.2 The electric and magnetic field components in LHM

Using Maxwell Equations, we get:

$$\nabla \times E = iwm_0 m_{eff}(w)H \tag{3.3}$$

$$\nabla \times H = iwe_0 e_{eff}(w)E \tag{3.4}$$

Where the effective permeability and the effective permittivity both are less than zero.

Considering the electric and magnetic field of TE wave propagation in the x-direction can be written as:

$$E = (0, E_y, 0)\exp[ik_0(bz - ct)] \tag{3.5}$$

$$H = (H_x, 0, H_z)\exp[ik_0(bz - ct)] \tag{3.6}$$

Where $b = \frac{k}{k_0}$ is the complex effective wave index constant, k_0 is the wave number of free space, and c is the velocity of light in free space.

The complex effective wave index constant can be written as:

$$b = \mathrm{Re}(b) + i\,\mathrm{Im}(b) \tag{3.7}$$

Where Re(β) is the reduced phase constant, and Im (β) is the reduced attenuation constant.

From Eq. (3.3) we get:

$$\begin{pmatrix} \hat{i} & \hat{j} & \hat{k} \\ ik & 0 & \dfrac{\partial}{\partial z} \\ 0 & E_y & 0 \end{pmatrix} = iwm_0 m_{eff}(w) \begin{pmatrix} H_x \\ 0 \\ H_z \end{pmatrix} \tag{3.8}$$

The components of the electric field and magnetic field are:

$$\frac{-\partial E_y}{\partial z} = iwm_0 m_{eff} H_x \tag{3.9}$$

From Eq. (3.9), we get:

$$H_x = \frac{i}{wm_0 m_{eff}} \frac{\partial E_y}{\partial z} \tag{3.9a}$$

Similarly,

$$ikE_y = iwm_0 m_{eff} H_z \tag{3.10}$$

From Eq. (3.10), we get:

$$H_z = \frac{k}{wm_0 m_{eff}} E_y \tag{3.10a}$$

Applying Eq. (3.4) then the components of magnetic field is:

$$\begin{pmatrix} \hat{i} & \hat{j} & \hat{k} \\ ik & 0 & \dfrac{\partial}{\partial z} \\ H_x & 0 & H_z \end{pmatrix} = -iwe_0 e_{eff}(w) \begin{pmatrix} 0 \\ E_y \\ 0 \end{pmatrix} \tag{3.11}$$

From Eq. (3.11) we get:

$$-\left(ikH_z - \frac{\partial H_z}{\partial z} \right) = -iwe_0 e_{eff}(w) E_y \tag{3.12}$$

$$-ikH_z + \frac{\partial H_z}{\partial z} = -iwe_0 e_{eff} E_y \tag{3.13}$$

Substitute both Eq's. (3.9a) and (3.10a) in Eq. (3.13) respectively, we obtain:

$$-ik\left(\frac{k}{wm_0 m_{eff}}\right)E_y+\frac{\partial}{\partial z}\left[\left(\frac{i}{wm_0 m_{eff}}\right)\frac{\partial E_y}{\partial z}\right]=-iwe_0 e_{eff}E_y \qquad (3.14)$$

Multiplying Eq. (3.14) by $\omega\mu_0\mu_{eff}$, we get:

$$-k^2E_y+\frac{\partial^2 E_y}{\partial z^2}=-w^2 e_0 m_0 m_{eff} e_{eff} E_y$$

$$\frac{\partial^2 E_y}{\partial z^2}-k^2E_y+w^2 m_0 e_0 m_{eff} e_{eff} E_y=0$$

$$\frac{\partial^2 E_y}{\partial z^2}-\left(k^2-w^2 m_0 e_0 m_{eff} e_{eff}\right)E_y=0 \qquad (3.15)$$

But $k_0^2=\frac{w^2}{c^2}$ where, $\frac{1}{c^2}=e_0 m_0$ (3.15a)

And $k = k_0\beta$ (3.15b)

Substitute both Eq's. (3.15a) and (3.15b) in Eq. (3.15), we obtain:

$$\frac{\partial^2 E_y}{\partial z^2}-\left(k_0^2 b^2-k_0^2 m_{eff} e_{eff}\right)E_y=0 \qquad (3.16)$$

Let $k_1^2=k_0^2\left(b^2-m_{eff}e_{eff}\right)$ (3.16a)

Finally, we get a second differential equation on the form:

$$\frac{\partial^2 E_y}{\partial z^2}-k_1^2E_y=0 \qquad (3.17)$$

The solution of Eq. (3.17) decays exponentially towards infinity and it becomes:

$$E_y = Ae^{k_1 z} \qquad (3.18)$$

Where, A is a constant and $k_1=k_0\sqrt{b^2-m_{eff}e_{eff}}$ (3.18a)

The relevant components of magnetic fields and the electric field in LHM have the form:

$$H_x^{(2)}=\frac{iBk_1}{wm_0 m_{eff}}e^{k_1 z}e^{i(k_1 x-wt)} \qquad (3.19)$$

$$H_z^{(2)}=\frac{Ak_1}{wm_0 m_{eff}}e^{k_1 z}e^{i(k_1 x-wt)} \qquad (3.20)$$

$$E_y^2 = Be^{k_1 z} e^{i(k_1 x - wt)} \tag{3.21}$$

With $k_1 = k_0 \sqrt{b^2 - m_{eff} e_{eff}}$ (3.21a)

But for TE-waves it can be shown that [22] there is a $\frac{p}{2}$ phase difference between H_x and H_z. It is converted to redefine the field components as:
$H_x = h_x$, $H_z = ih_z$ and $E_y = ie_y$, so the field components can be written in the left handed material cover as:

$$H_x^{(2)} = \frac{iBk_1}{wm_0 m_{eff}} e^{k_1 z} e^{i(k_1 x - wt)} \tag{3.22}$$

$$H_z^{(2)} = \frac{iBk_1}{wm_0 m_{eff}} e^{k_1 z} e^{i(k_1 x - wt)} \tag{3.23}$$

$$E_y = iBe^{k_1 z} e^{i(k_1 x - wt)} \tag{3.24}$$

3.3 Boundary conditions

Applying the boundary conditions for the continuity of tangential H at z = 0 and from Eq. (3.2a) and Eq. (3.22), we get:

$$h_x^{(1)} = H_x^{(2)} \tag{3.25}$$

$$ikAe^{kz} e^{i(kx - wt)} = \frac{iBk_1}{wm_0 m_{eff}} e^{k_1 z} e^{i(k_1 x - wt)}$$

at z = 0

Then, we have:

$$kAe^{i(kx - wt)} = \frac{Bk_1}{wm_0 m_{eff}} e^{i(k_1 x - wt)} \tag{3.26}$$

The second boundary condition yields,

$$e_y^{(1)} = E_y^{(2)} \tag{3.27}$$

at z = 0

$$-iwm_0 A(Sm_{xz} + m_{xx}) e^{kz} e^{i(kx - wt)} = iBe^{k_1 z} e^{i(k_1 x - wt)}$$

Then we get:

$$-wm_0 A(Sm_{xz} + m_{xx})e^{i(kx-wt)} = Be^{i(k_1x-wt)} \tag{3.28}$$

Dividing Eq. (3.26) by Eq. (3.28) we obtain:

$$\frac{kAe^{i(kx-wt)}}{-wm_0 A(Sm_{xz} + m_{xx})e^{i(kx-wt)}} = \frac{Bk_1 e^{i(k_1x-wt)}}{wm_0 m_{eff} Be^{i(k_1x-wt)}}$$

Simplify the above equation, we get:

$$\frac{k}{-(Sm_{xz} + m_{xx})} = \frac{k_1}{m_{eff}}$$

Then,

$$\frac{k}{k_1} = \frac{-1}{m_{eff}}(Sm_{xz} + m_{xx}) \tag{3.29}$$

With,

$$k_1 = k\sqrt{b^2 - e_{eff} m_{eff}} \tag{3.29a}$$

$$k = k_0\, \beta \tag{3.29b}$$

Substitute Eq's. (3.29a) and (3.29b) in Eq. (3.2a) we obtain:

$$\frac{k_0 b}{k_0\sqrt{b^2 e_{eff} m_{eff}}} = \frac{-1}{m_{eff}}(Sm_{xz} + m_{xx})$$

$$b = -\sqrt{\frac{b^2 - e_{eff} m_{eff}}{m_{eff}^2}}(Sm_{xz} + m_{xx})$$

By squaring both sides then,

$$b^2 = \left(\frac{b^2}{m_{eff}^2} - \frac{e_{eff} m_{eff}}{m_{eff}^2}\right)(Sm_{xz} + m_{xx})^2$$

$$b^2 = b^2\left(\frac{1}{m_{eff}^2} - \frac{e_{eff}}{b^2 m_{eff}}\right)(Sm_{xz} + m_{xx})^2$$

$$1 = \frac{(Sm_{xz} + m_{xx})^2}{m_{eff}^2} - \frac{e_{eff}(Sm_{xz} + m_{xx})^2}{m_{eff} b^2}$$

$$\frac{e_{eff}}{b^2 m_{eff}}(Sm_{xz} + m_{xx})^2 = \frac{(Sm_{xz} + m_{xx})^2}{m_{eff}^2} - 1$$

$$\frac{1}{b^{2}}=\frac{m_{eff}\left(Sm_{xz}+m_{xx}\right)^{2}}{e_{eff}\,m_{eff}^{2}\left(Sm_{xz}+m_{xx}\right)^{2}}-\frac{m_{eff}}{e_{eff}\left(Sm_{xz}+m_{xx}\right)^{2}}$$

$$\frac{1}{b^{2}}=\frac{1}{e_{eff}\,m_{eff}}-\frac{m_{eff}}{e_{eff}\left(Sm_{xz}+m_{xx}\right)^{2}}$$

$$\frac{1}{b^{2}}=\frac{\left(Sm_{xz}+m_{xx}\right)^{2}-m_{eff}^{2}}{e_{eff}\,m_{eff}\left(Sm_{xz}+m_{xx}\right)^{2}}$$

Finally,

$$b^{2}=\frac{e_{eff}\,m_{eff}\left(Sm_{xz}+m_{xx}\right)\,\left(Sm_{xz}+m_{xx}\right)}{\left(Sm_{xz}+m_{xx}\right)\,\left(Sm_{xz}+m_{xx}\right)-m_{eff}^{2}} \tag{3.30}$$

This is the required general dispersion relation which defines the propagation of the magnetostatic surface waves between ferrite cladding and left-handed material. It has two solutions for ω(k), one represents a physical solution and other is unacceptable. However, Eq. (3.30) is numerically analyzed by using software program and plotting dispersion curves (a) forward (b) backward, which are the relation between ω(k) and β.

4.1 Data and calculations

In the previous chapter we got on a dispersion relation that represents the guiding structure between a linear semi-infinite ferrite substrate assumed to be YIG, and a left-handed material cladding. Hence, in order to make a numerical analysis we need some computations concerns with the two media.

Firstly, for the data parameters of linear ferrite (YIG), we used the data given by Shabat [13] as $\mu_0 H_0$ = 0.1 T , μ_B = 1.25 , $\mu_0 M_0$ = 0.1750 T , $\gamma = 1.76 \times 10^{11}$ rad S^{-1} T^{-1} to compute both components μ_{xx} and μ_{xz} of permeability tensor media.

Secondly, with respect to left-handed material, we used the data given by Ruppin [7] as $\frac{w_p}{2p} = 10$ GHz for calculating the effective permittivity ε_{eff}, $\frac{w_0}{2p} = 4$ GHz and the constant F = 0.56 for calculating the effective permeability μ_{eff}.

4.2 Numerical results and discussion

In the region of interest, where we deal with magnetostatic surface waves, for $m_v \leq 0$,we took the frequency in the range from $\sqrt{f_0(f_0 + f_m)}$ to $(f_0 + f_m/2)$ and upon the previous data it was 4.6 GHz to 5.8 GHz. Since, $S = \pm 1$, where $S = 1$ for the propagation in the forward direction, and $S = -1$ for the backward direction.

Hence, we noticed that the derived nonlinear dispersion equation (3.30) has two different solutions, depending upon the direction of propagation or the direction of external applied magnetic field. One solution is acceptable and other represents a non-physical solution for ω(k).

Numerical computations were carried out considering the same parameters were taken with respect to the substrate (YIG) and LHM-cladding. We noticed that the only solution exists in the region 4<f<6 (GHz), where the refractive index is expected to take a negative value and both the permittivity and the permeability have negative values (ε <0, μ<0).

Moreover, Fig.(4.1) shows the linear dispersion curves which is the variation of the frequency with the wave index are display the (*i*) expected reciprocal behavior, which is important in microwave signal processing technology, (*ii*) since the propagation characteristics both forwards to the right and symmetrical (β>0). So, this back to the derived quadratic dispersion equation (3.30), (*iii*) the frequency is decreasing with increasing the wave number k and this happen only in the propagation of TE-magnetostatic surface waves.

Also, we increase the value of the applied external magnetic field $\mu_o H_o$ by 0.52T, 0.55T and 0.6T respectively. Its seen that the propagation of TE-magnetostatic surface waves disappeared in the proposed region and this back to the change of the permeability tensor components μ_{xx}, μ_{xz} in our derived dispersion relation (3.30). So, this make the guiding structure loses its LHM-characteristics in the region 4 < *f* < 6 (GHz).

Similarly, we increase the values of the plasma frequency ω_p greater than $\frac{w_p}{2p} = 10GHz$ and the value of resonance frequency ω_o greater than $\frac{w_o}{2p} = 4GHz$ with F(constant)=0.6 in calculating μ_{eff}, ε_{eff} respectively, it noticed that the propagation of TE-magnetostatic surface waves disappeared in the proposed region.

In general, due to the above discussion we conclude that the guiding structure have only a particular range which is the guiding structure transmit a TE-magnetostatic surface waves as shown in fig.(4.1).

Finally, we examined the behavior of magnetostatic surface waves outside the proposed region which is , where the refractive index is expected to take a non-negative value in this interval considering the region of the interest $m_v < 0$. We noticed that there are two special cases which is:

Case I:

In the region *f*<4(GHz) where $m_v > 0$ and $e < 0$, the LHM medium is transparent medium and the guiding structure becomes a metallic fig.(4.2a) [23].

On the other hand we increased the applied external magnetic field $\mu_o H_o$ for both forward and backward wave propagation by the values 0.2T and 0.3T, we noticed that the propagation in the forward direction began to decrease as shown in fig.(4.2b) and fig.(4.2c) respectively.

Case II:

In the region *f* >6 (GHz) where ($m_v > 0, e > 0$), we noticed that there are two ranges:

Firstly, in the range 6 < *f* < 10 (GHz), there is no physical solution for the dispersion equation (3.30).

Secondly, however after the frequency of 10 GHz, the physical solutions are starting to appear and the guiding structure becomes a dielectric as shown in fig.(4.3a).

Similarly, we increased the applied external magnetic field $\mu_o H_o$ for both forward and backward wave propagation in this region by the values 0.2T and 0.3T. It is seen that the propagation in the forward direction began to disappear as seen in fig.(4.3b) and fig.(4.3c) respectively.

4.3 Conclusions

The dispersion propagation characteristics of nonlinear magnetostatic surface waves through various waveguide structures containing linear ferrite (YIG) and (LHM) layers are investigated.

Moreover, the dispersion relations for electromagnetic waves are derived for each waveguide structures by using Maxwell's equations and the boundary conditions. Both figures show the nonreciprocal behavior in the graphs.

In addition, in the region for $f < 4$ GHz , the guiding structure behaves as a metal, while in the region $f \geq 10$ GHz behaves as a dielectric.

Finally, the study of nonlinear optical effects in various waveguide structures containing YIG with LHM media is considered a key problem of the simulation of a number of opto-microwave electronic devices. So, it is hoped that this work will act as a motivation for future studies in this area.

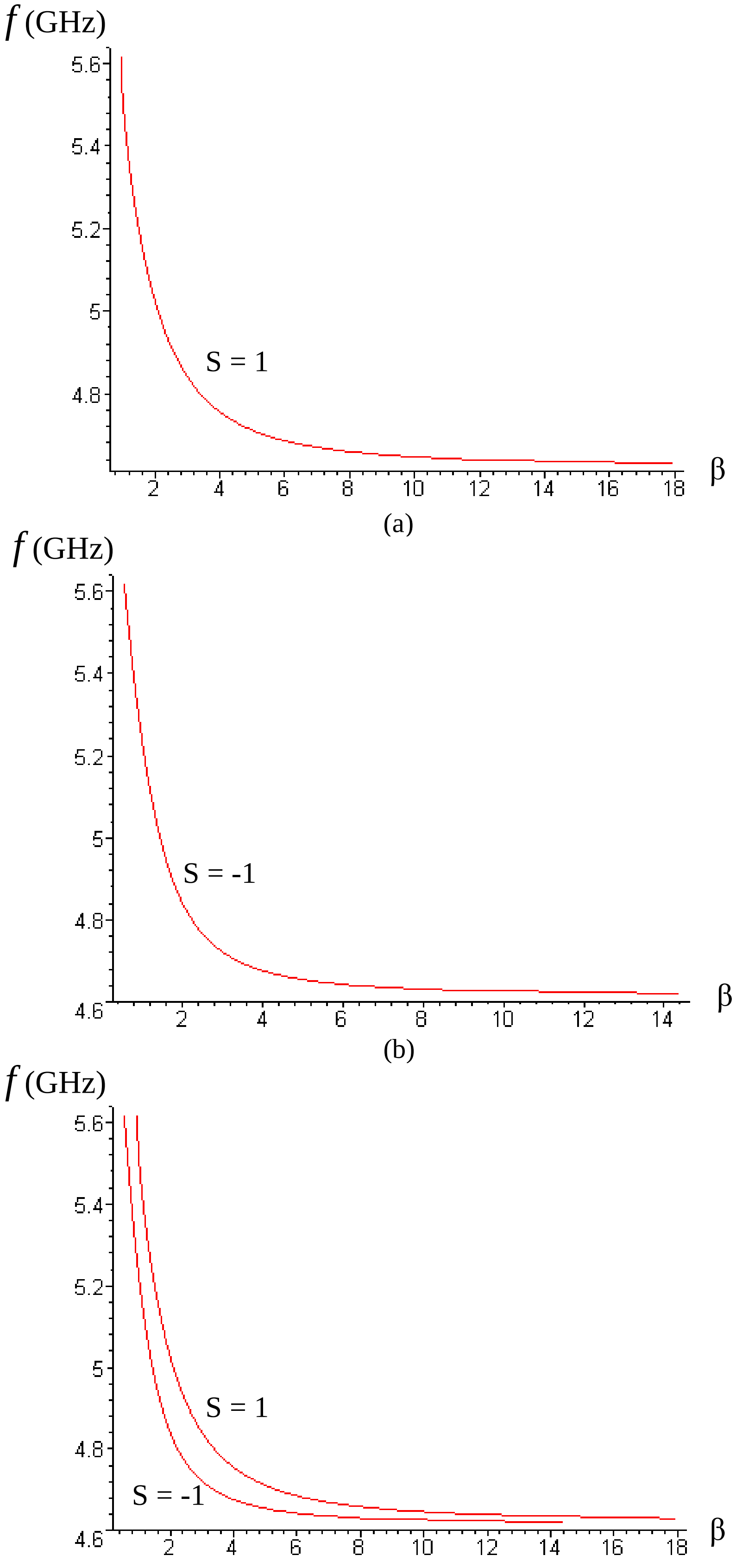

Fig. (4.1): shows the computed dispersion curves in (a) forward, (b) backward and (c) both wave propagation. $\mu_0 H_0 = 0.05$ T, $\mu_B = 1.25$, $\mu_0 M_0 = 0.1750$ T, $\gamma = 1.76 \times 10^{11}$ rad s^{-1} T^{-1},

$\frac{w_p}{2p} = 10\ GHz$, $\frac{w_0}{2p} = 4\ GHz$, F = 0.56

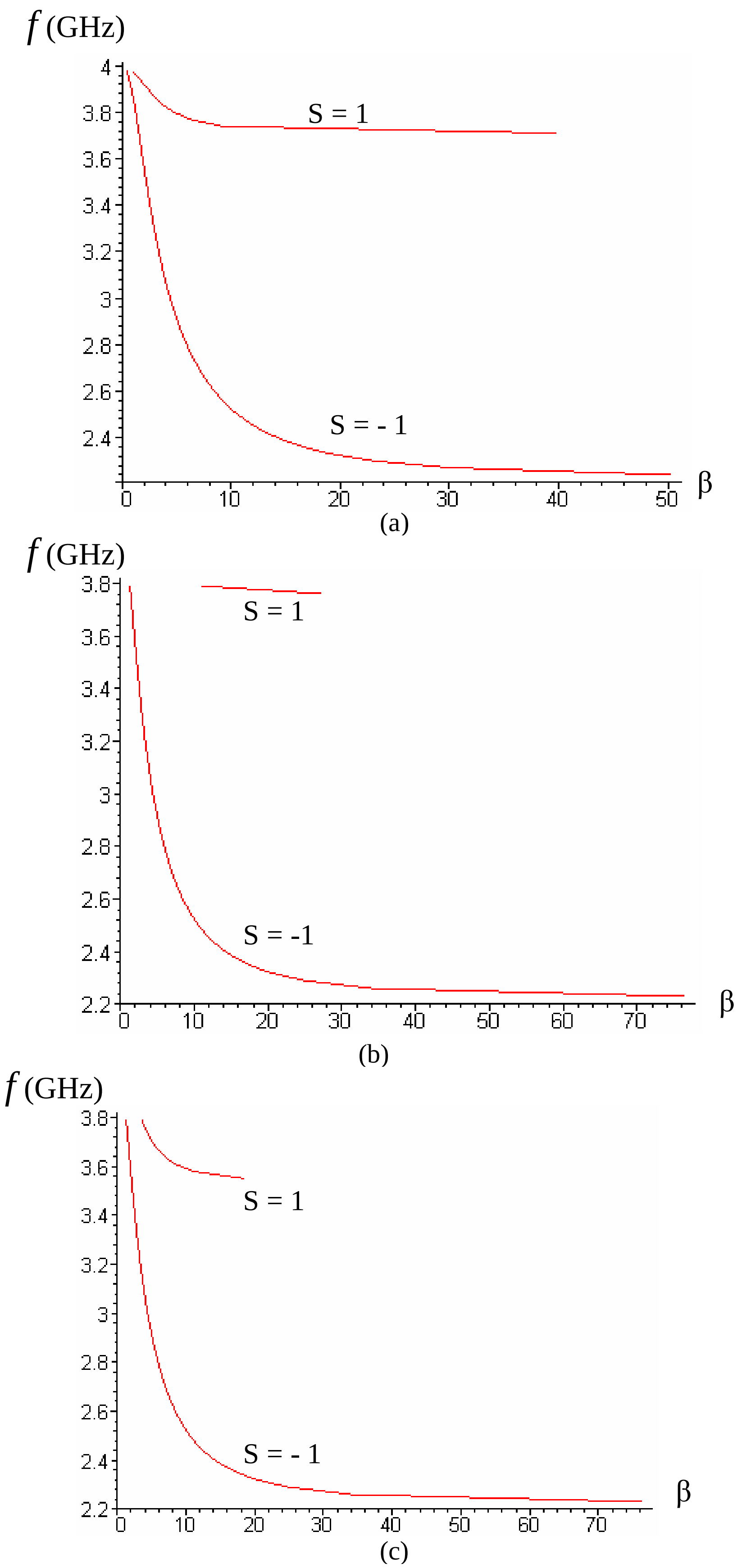

Fig. (4.2): shows the Guiding structure considered as a metal in all regions in case ($f < 4$ GHz), $\mu_0 H_0$ = 0.05 T, 0.2T, 0.3T, μ_B = 1.25, $\mu_0 M_0$ = 0.1750 T, $\gamma = 1.76 \times 10^{11}$ rad s^{-1} T^{-1},

$\frac{w_p}{2p} = 10 \;\; GHz$, $\frac{w_0}{2p} = 4 \;\; GHz$, F = 0.56

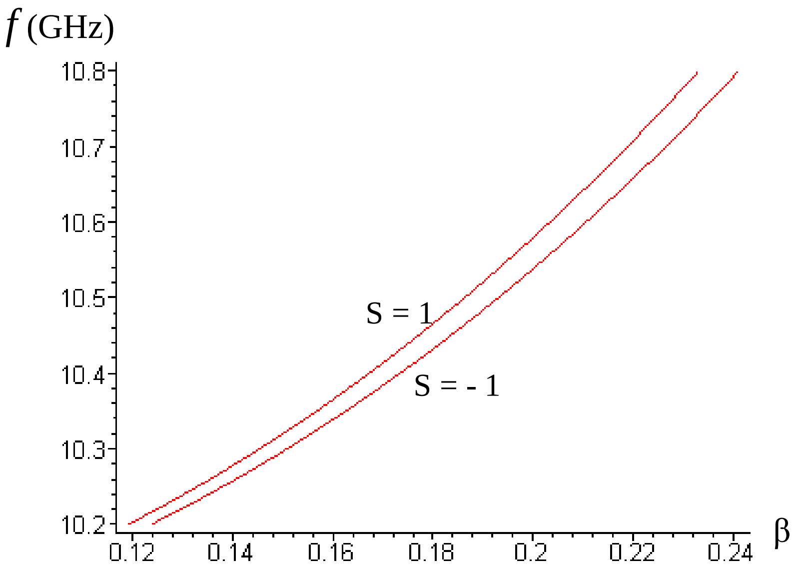

(a)

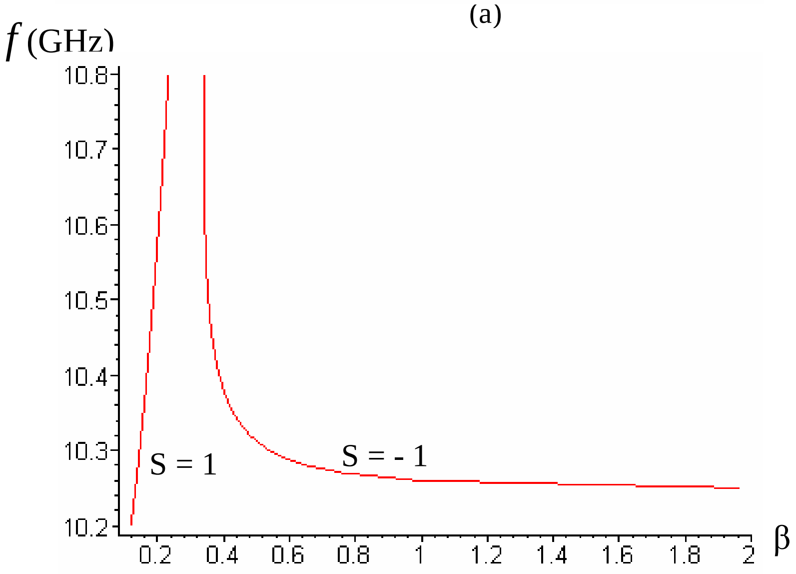

(b)

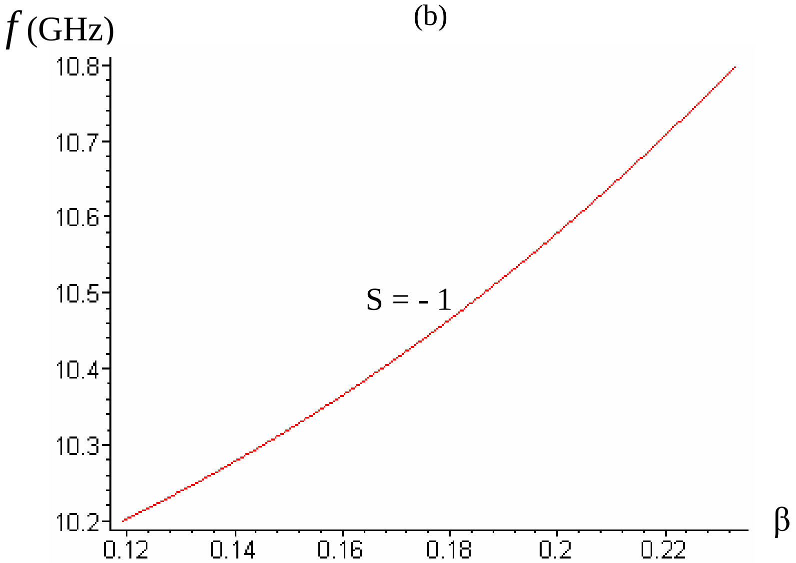

(c)

Fig. (4.3): shows the Guiding structure considered as a dielectric in all regions in case ($f > 6$ GHz), $\mu_0 H_0 = 0.05$ T, 0.2 T, 0.3 T, $\mu_B = 1.25$, $\mu_0 M_0 = 0.1750$ T, $\gamma = 1.76 \times 10^{11}$ rad s^{-1} T^{-1},

$\frac{w_p}{2p} = 10\ \ GHz$, $\frac{w_0}{2p} = 4\ \ GHz$, F $= 0.56$

REFERENCES

1. V. G. Veselago, Sov. Phys. Usp. 10, 509, (1968).
2. Smith, D. R., P. Rye, D. C. Vier, A. F. Starr, J. J. Mock, T. Perram, "Design and Measurement of Anistropic Meatamaterials that Exhibit Negative Refraction", IEICE TRANS. ELECTRON., Vol. **E87 – C**, No. 3, (2004).
3. Smith, D. R., W. J. Padilla, D. C. Vier, S. C. Nemat – Nasser and S. Schultz, "Composite Medium with Simultaneously Negative Permeability and Permittivity", Phys. Rev. Lett., Vol. **84**, No. 18, 4184, (2000).
4. R. A. Shelby, D. R. Smith, S. Schultz, Science 292, 77 (2001).
5. J. B. Pendry, S. A. Ramarkrishna, J. Phys.: Cordens. Matter 14, 6345 (2003).
6. J. B. Pendry, A. J. Holden, D. J. Robbins, W. J. Stewart, IEEE Trans. Microwave Theory Tech. 47, 2075, (1999).
7. R. Ruppin, J. Phys. Condens. Matter, Vol. **13**, 1811 – 1819, (2001).
8. A. V. Vashkovskii and E. G. Lokk "Magnetostatic Surface Waves in a Ferrite-Dielectric Structure Bounded by Half-Spaces with Negative permittivity" J. phys., Vol. **47**, No. 1, 87 – 91, (2002).
9. Further reading can be found in a special of Opt. Express, "Focus Issue: Negative Refraction and Metamaterials" **11**, 639 – 755 (April 2003), and in M. W. McCall, A. Lakhtakia, W. S. Weiglhofer, Eur. J. Phys. **23**, 353, (2002).
10. I. W. Shadrivov, A. A. Sukhrukov, and Y. S. Kivshar, "Guided modes in negative-refractive-index waveguides" Phys. Rev. E, Stat. phys. plasmas Fluids Relat. Interdiscip. Top., Vol. **67**, No. 5, 057602 – 057602, May 2003.

11. M. S. Hamada, M. M. Shabat and D. Jäger "Nonlinear TM surface waves in a left-handed material structure" Proceeding of SPIE, Vol. **5445**, P 184-186, (2003)
12. Damon, R. W. and J. R. Eshbach, "Magnetostatic modes of ferromagnetic slab", J. phys. Chem.. solids, vol. 19, 308, 1961.
13. M. M. Shabat, "Nonlinear Magnetostatic Surface Waves in a gyromagnetic film" philosophical Magazine B, Vol. **73**, No. 4, 669 – 676, (1996).
14. M. M. Shabat, "Strongly Nonlinear Magnetostatic Surface Waves in a Grounded Ferrite Film" phys. Stat. Sol. (a) **149**, 691 (1995).
15. D. H. Staelin, A.W. Morgenthaler and J. A. Kong "Electromagnetic Waves" (Prentice-Hall International, Inc. 1994).
16. J. D. Jackson "Classical Electromagnrtics" (John Wiley & Sons, Inc. 1975).
17. E. C. Jordan and K. G. Balmain, "Electromagnetic Waves and Radiating Systems" (Prentic-Hall, Englewood cliffs, NJ, 1968).
18. A. D. Boardman, M. M. Shabat and R. F. Wallis "Nonlinear Magnetodynamic Waves on Magnetic Materials" Physical Review B, Vol. **41**, No. 1, 717 – 730, (1990).
19. A. D. Boardman, M. M. Shabat and R. F. Wallis "TE waves at an interface between linear gyromagnetic and nonlinear dielectric media" J. Phys. D: Appl. Phys. **24**, 1702-1707, (1991).
20. M. I. Kaganov, N. B. Pustyl'nik, and T. N. Shalaeva "Magnons, magnetic polaritons, magnetostatic waves" physics – Uspekhi **40** (2) 181 – 224, (1997).
21. A. D. Boardman, M. Bertolott and T. Twardowski "Nonlinear Waves in Solid State Physics" Plenum Press, New York, (1990).

22. M. M. Shabat and J. Pelzl, "Nonlinear Electromagnetic Surface Waves in the magnetic structure" Infrared Physics & Thechnology **37**, 265 – 270, (1996).
23. A. Hartestein, E. Burstein, A. A. Maradudin, R. Brewer and R. F. Wallis "Surface Polaritons on semi-infinite gyromagnetic media" J. phys. C: Solid state phys., Vol. **6**, (1973).
24. K. M. Heal, M. L. Hansen and K. M. Rickard "Maple V: Learning Guide" (Waterloo Maple Inc., 1998).

الملخص العربي

أثر الموجات الاستاتية المغناطيسية الغير خطية
على مواد ذات السماحية و النفاذية السالبة معاً

من الملاحظ خلال السنوات القليلة الماضية، وجود العديد من الدراسات حول انتشار الموجات الكهرومغناطيسية غير الخطية وكذلك الموجات الاستاتية المغناطيسية الغير خطية عبر رقائق من مواد تسمى LHM's ذات السماحية و النفاذية السالبة معاً.

كما أن اكتشاف هذه المواد و استخدامها في بعض التطبيقات العملية مثل صناعة الاتصالات الخلوية، الهوائيات و التنقية Filtering وبعض الأجهزة الكهرومغناطيسية البالغة الأهمية له الأثر الكبير في إثارة اهتمام الباحثين بهذا المجال.

لقد قمنا بدراسة تحليلية لمعرفة خصائص ومميزات و تشتت الموجات الاستاتية المغناطيسية الغير خطية (nonlinear magnetostatic surface waves) خلال طبقتين من مادة الفريت (YIG) و الأخرى مادة (LHM) بخصائصها المعروفة عن طريق استخدام معادلات ماكسويل، والشروط الحدية واشتقاق معادلة الخصائص والتشتت (dispersion equation) لتحديد ثابت الانتشار المركب بطريقة التحليل العددي.